Experimental and theoretical investigation into surface roughness and residual stress using ball end magnetorheological finishing

DOI : 10.36909/jer.14281

Anand Sharma*, Mahendra Singh Niranjan*

**Department of Mechanical Engineering, Delhi Technological University, Delhi, India*

Corresponding Author: doc.asharma@yahoo.in

ABSTRACT

The generation of residual stresses by grinding process on the surface for a soft material results in poor performance and diminished life. In this paper, grinding-induced residual stresses is addressed and an attempt is made to relieve these residual stresses while achieving nano level surface finish using ball end magnetorheological finishing (BEMRF) process. BEMRF is a recently developed process that is effectively used to for fine figuring and polishing of a variety of magnetic and non-magnetic materials. In our present work we will demonstrate the relieving of residual stresses and reduction in surface roughness generated after surface grinding of Aluminium 7075 workpiece using BEMRF process. The impact of various BEMRF variables on reduction in surface roughness and residual stresses are discussed statistically and graphically. Residual stresses of workpiece surfaces have been measured by using portable X-ray residual stress analyzer. Significant process parameters affecting the residual stresses during polishing of workpiece are obtained using Analysis of variance (ANOVA) and F-test. It has been observed that reduction in residual stress is achieved along with nano level surface finish on aluminium workpiece surface using BEMRF technique.

Keywords: Residual stress; nanofinishing; magnetorheological; aluminium; ANOVA

INTRODUCTION

In this age of new industrialization revolution, there is a high demand for both nano products and macro products with high surface finish and strength (Li, 2020). Arun et al., 2021; Mahadik et al., 2020 & Qiu, 2021 discussed various applications of nano products in the field of biomedical and solar cells. However, development of gigantic Airbus A380 mostly with aluminium alloy confirms that this material possesses properties like high hardness, toughness, strength to weight ratio values etc. that are required in today's advanced industries. While achieving the best out of the aluminium alloys sometimes unwanted residual stresses are generated on the workpiece surface which leads to sub-surface damage resulting in part distortion. Brinksmeier (2007) observed that the various types of material processing methods, complex component design and

manufacturing techniques causes high residual stresses to be induced in the workpiece surface resulting in part distortion. Sim (2010) described that every year millions of Euros are spent trying to improve the quality of parts or components specially in aerospace industries by removing or avoiding such distortions. Ghosh (2021) mentioned in the article that even sometimes while polishing of workpiece, some amount of residual stresses is induced on workpiece surfaces leading to alteration in inter-planar spacing which directly influences the reflectivity and refraction index of polished product to be used in optical applications. Tyagi (2002) investigated the effect of residual stress on the optical properties of cadmium iodide films. The results showed that the residual stress was increased nonlinearly with thickness of the film and temperature of the treatment whereas a linear decrement in residual stress was observed with substrate temperature. Yi (2011) theoretically and experimentally explained the controlling of compression molding process through proper cooling in order to control the residual stresses which affects the glass properties. Sugano (1987) experimentally showed that an unwanted compressive residual stress of 60 MPa was induced during the diamond turning of aluminium alloy which resulted in sub-surface damage. Residual stresses are generally undesirable stresses that are developed in a workpiece after machining. Upon removal of such unwanted stresses can enhance the functional behavior and efficiency of machined components.

Being one of the most popular machining methods for hard materials the grinding process directly influences the operational properties of the workpiece such as fatigue strength, abrasive and corrosion resistance etc while creating a new surface of the workpiece. Achieving favourable surface integrity while obtaining high productivity during grinding process leads to a serious damage to the surface layer. Due to the high importance of grinding process, various investigations have been made to find a compromise between high productivity and favourable surface layer. Some approaches are analytical in nature which are based on the mathematical calculations of temperature distribution in the workpiece helping in the estimation of microhardness, residual stresses, microstructure etc. Kruszynski (1991) analytically analyzed the damage to the surface layer of the metal by grinding process through creation of residual stress keeping a close view of thermal aspects of grinding. It was concluded that the new proposed grinding parameter combining depth of cut, work speed and wheel speed have better control on the surface integrity during industrial practice. Tönshoff (1992) modeled and simulated the grinding energy and force models during grinding process. Also, kinematic and energetic processes were taken into consideration for temperature and surface integrity models. Brinksmeier (1987) established a model signifying that the generation of residual stresses depends on the machining parameters and selection of grinding wheel. Other approaches are purely experimental aiming at discovering the

best possible relationship between grinding and surface quality parameters. Zhejun (1989) investigated the surface integrity of grinding of hardened bearing steel. Results showed that the compressive residual stresses and harmful tensile residual stresses are formed when cubic boron-nitride wheels and aluminium oxide wheels are used respectively. Robinson (2010) measured residual stress distribution in 7449 aluminium alloy through neutron diffraction and deep hole drilling. Results of the neutron diffraction showed that a large amount of tensile residual stresses were formed at the centre of the quenched forging which was balanced by a compressive residual stress on surface region. Jomaa (2014) investigated the surface finish and development of residual stresses during orthogonal cutting of AA7075-T651 alloy under dry conditions. Results showed that with increase in cutting speed the residual stresses were tensile on surface. Lambropoulos (2001) demonstrated the issue of grinding-induced stresses and deformation in commercial Si wafers and removal of these stresses using non-conventional magnetorheological finishing (MRF) method. The results showed that by MRF polishing 90-95% of the residual stresses are relieved. Arrasmith (2001) introduced compressive surface stress by lapping 100mm diameter silicon wafer with different alumina abrasive particles and subsequently polished using magnetorheological finishing technique for relieving of induced stresses. Results showed that MRF technique successfully removed the surface grinding force for silicon wafer lapped with 5µm alumina abrasives.

Aluminium alloys are extensively used in semi-conductor manufacturing, specific purpose telescopes, optical systems and sensors, micro-electronic devices and at an enormous extent for conduction through wires. Koul (2011) made diamond cut aluminum based mirrors to be used as light collector in a specific telescope at Hanle, a high altitude astronomical site in India. Jaecklin (1994) experimentally observed the optical properties such as surface reflectivity and scattering characteristics of aluminum based micro mirrors along with two other materials such as single-crystal silicon and polycrystalline silicon and their mechanical properties. Results showed that the mirrors made of aluminum had higher surface reflectivity. Ahn (2004) polished aluminium surface through chemical mechanical polishing process which is increasingly used for developing MEMS using silica based slurry. However, apart from the properties mentioned above possessed by aluminium alloys they are also very ductile, malleable and poorly resistant to scratching behaviour which hinders the aim of achieving nano level surface finish. Chiu (2003) mentioned that it is a challenge to obtain good structural planarity and minimum surface scratching during chemical mechanical polishing of aluminum due to its soft nature. Considering low resistivity to scratching of aluminium, it becomes difficult to achieve nano level surface finish without damaging the surface integrity using conventional finishing processes. Vahdati (2008) found that various

finishing constraints such as finishing tool rotation, duration of finishing, type of abrasives, distance between magnetic tool & workpiece, lubricant used and finishing forces acting on the workipece can influence the removal rate of material and finish of the surface. Khan (2019) observed that the fluid composition especially the abrasive mesh size is an important parameter for finishing soft material like copper. Zhong (2003) found conventional process like turning of workpiece through single-point diamond also known as SPDT to be an efficient method to attain nanometric finish on soft materials such as copper, aluminium etc. but it is difficult to control the finishing forces.

Keeping in view the limitation of conventional finishing processes, various non-conventional finishing methods like magnetorheological fluid finishing (MRF), magnetorheological abrasive flow finishing (MRAFF), Chemo-mechanical magnetorheological finishing (CMMRF) etc. have been developed which controls the finishing forces using magnetic field to attain high surface finish. Jacobs (1995) described MRF process for finishing of optical components. Experimental results demonstrated that this process can be used to finish both spheres and aspheres optical glasses.

Golini (1997) experimentally finished a variety of spherical, flat, aspheres optical materials with two different machine configurations through MRF process. Results showed that the MRF process is highly capable of finishing optical materials, correcting figure errors without leaving any sub-surface damage to the workpiece.

Jha (2004) developed MRAFF process for finishing of complex internal geometries. To observe the performance of the process, surface roughness of stainless steel workpieces was referred as main output response. Magnetic flux density was varied from 0 to 0.574 Tesla to study the variation in surface roughness. Results showed that the surface roughness was reduced from 0.49μm to 0.34μm when the magnetic flux density value was fixed at 0 and 0.575 Tesla respectively. Also, at higher magnetic flux density the depths of grinding marks were reduced.

Jain (2010) made an effort in designing a finishing process (CMMRF) which combines the advantageous features of chemical mechanical polishing (CMP) and MRF for achieving nano level surface finish of silicon blanks with minimum surface damage and high material removal rate. Silicon blanks were polished in four stages with MR fluid containing silicon carbide, cerium oxide abrasives and magnetic particles mixed in water and oil base. It was observed that surface finish of 4.8Å was obtained through this process.

The limitations of finishing restricted geometries such as convex, curved in, plane and aspherical due to the constraint in relative motion of workpiece and finishing tool, were surpassed by developing BEMRF process a recently advanced version of MRF method. Singh (2012)

validated the BEMRF process developed by finishing EN31 and copper workpieces experimentally and simulating the magnetic flux density between the tool and workpiece. It was demonstrated that the performance of the newly developed process depends on magnetic nature of the workpiece, working gap and magnetizing current as EN31 workpiece obtained a surface finish of 70nm whereas surface finish of copper workpiece reached to a value of 102nm. Simulation of magnetic flux showed that the shape and size of the ball-end finishing spot varied with the working gap at particular magnetic current. Sharma (2019) critically reviewed MRF, MRAFF, CMMRF, BEMRF finishing process and concluded that BEMRF process is an effective process to obtain high level of surface finish on variety of work pieces. Sharma (2020) reviewed in detail the BEMRF process and concluded that this process can be effectively used for finishing of both magnetic and non-magnetic materials.

It has been observed from the past studies that the reduction of surface roughness and residual stress induced on aluminium alloy after grinding are rarely discussed. In this paper, high surface irregularity and residual stresses induced by grinding in the aluminium 7075 surface and subsequent polishing by BEMRF process resulting in reduction of residual stresses and surface roughness is discussed. Maloney (2016) observed that the ball end magnetorheological finishing (BEMRF) process based on smart fluids have an ability to control the finishing forces which enables it to finish 3D surfaces to nanometer levels without imposing surface or sub-surface damage to the finished component. This process is capable of finishing and polishing a variety of materials, either magnetic materials like diverse alloys of steel etc., or nonmagnetic materials such as glass, silicon, aluminum, copper, etc. Singh (2012) finished fused silica glass workpiece using computer numerically controlled BEMRF process for achieving nanometric level surface finish without sub-surface damage. A minimum of 0.14nm arithmetical mean roughness was obtained after finishing four times for 30 minutes each. Deep scratches on the workpiece surface were also observed when the applied magnetizing current was at a level of 4 amperes in first experiment. However, the magnetizing current was reduced to 2.4 amperes which resulted in much improved surface quality. Saraswathamma (2015) experimentally observed the effect of tool rotational speed, gap between the tool and workpiece and magnetizing current on surface roughness of silicon wafer during BEMRF process. Obtained results exhibited that on increasing the working gap decreases the surface finish whereas an increase in magnetizing current increases the surface finish of the silicon wafer. Also, surface finish decreased with increase in tool rotation at higher working gap. Khan (2018) finished non-magnetic copper workpiece through BEMRF process and simulated the magnetic flux density between the workpiece and the finishing tool which was then verified experimentally. Optimized MR fluid was also synthesized to obtained best results during

finishing of copper workpiece. It was observed that the magnetic flux density between the tool and the workpiece was significantly increased from 0.35 to 0.85 Tesla when copper was placed above a permanent magnet for creating two opposite magnetic poles which lacked before the introduction of permanent magnet due to copper being non-magnetic in nature.

The setup of BEMRF included vertically oriented MR finishing tool driven by servo motor comprising of cylindrically shaped inner core (made of iron), an outer core oriented concentrically to each other and electromagnetic coil (Figure 1(a)). The designing of electromagnet coil is done keeping in view to attain magnetic flux density not less than ~0.8 T at the MR finishing tool tip and is surrounded by copper tube through which chilled water is circulated to maintain the setup at a suitable temperature. The delivery of MR fluid was controlled by a delivery pump from the storage tank (funnel shape) to the tool tip. Figure 1(b) represents the development of a nearly ball shaped highly viscous MR fluid at the tool tip. As soon the MR fluid reaches the tip of the finishing tool, the magnetic CI particles present in the MR fluid aligns themselves along the magnetic field flow direction. The viscosity of the MR fluid is controlled or varied by regulating the power supply or current hence controlling the magnetic field strength.

The effectiveness of BEMRF process is highly affected by the magnitude and distribution of the magnetic flux density around the finishing region. Kansal (2018) invested during BEMRF of diamagnetic material the tip of the tool acts as a single pole and due to lack of opposite magnetic pole the deviation of magnetic flux lines take place which reduces the magnetic strength resulting in low material removal rate. In order to avoid the deviation of magnetic flux lines, a permanent magnet was placed under the workpiece so as to direct the magnetic flux through the non-magnetic material.

EXPERIMENTATION

In the present study, the effect of BEMRF input process parameters viz. magnetizing current (V_M), tool rotation (T_R) and working gap (W_X) on percentage surface roughness reduction (%SRR) and percentage reduction in residual stresses (%RRS) has been discussed. Table 1 presents the levels of the selected input parameters based on the preliminary experiments conducted and the parameters to be kept constant. Initial and final surface roughness values of workpiece were measured at five places using Mitutoyo Surftest SJ-301 before and after finishing through BEMRF process. Residual stresses initially induced after grinding procedure in aluminium 7075 workpieces and final residual stresses after BEMRF were measured using X-Ray residual stress analyzer. The residual stresses can be measured efficiently by detecting the full Debye ring data from a single incident X-ray angle.

According to Box-Behnken design technique, 17 experiments had to be conducted varying the input process parameters at three different levels. The experiments were conducted on 3-axis CNC BEMRF setup as shown in figure 1(a). Table 2 indicates the run order for performing of experiments, initial and final values of surface roughness and residual stresses and output responses i.e. percentage reduction in surface roughness (%SRR) and residual stresses (%RRS) for each specimen.

Table 1. Levels and ranges of selected process parameters

Process parameter	Units	Levels			Static Parameters	Description
		I	II	III		
Magnetizing Current (V_M)	amp	1.5	2.5	3.5	Feed Rate	5 mm/min
Tool rotation (T_R)	rpm	300	500	700		
Working gap (W_X)	mm	0.5	1.5	2.5		

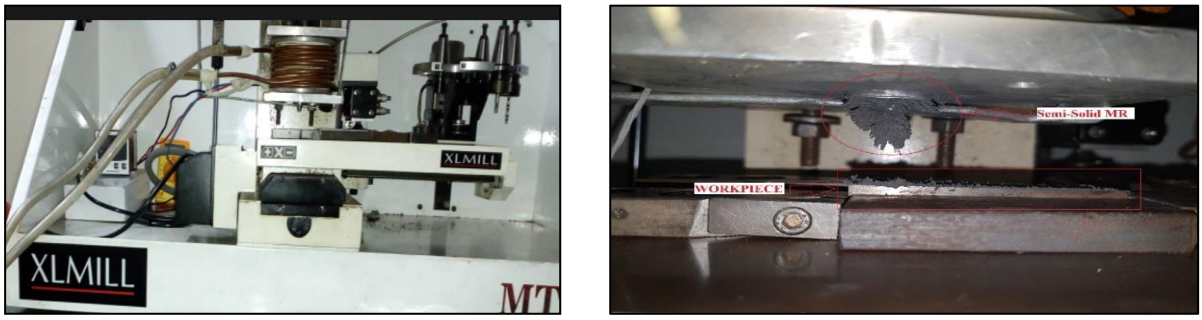

(a) (b)

Figure 1. (a) setup of BEMRF tool and (b) semi-solid MR ball formation

Table 2. Design of experiments and output responses

Input Process Parameters					Initial Surface Roughness	Final Surface Roughness	Output Response 1	Initial Residual Stress	Final Residual Stress	Output Response 2
Std Order	Run Order	V_M	T_R	W_X	SR_i (nm)	SR_f (nm)	%SRR	RS_i (MPa)	RS_f (MPa)	% RRS
1	15	1.5	300	1.5	825	491	40.48	124	55	55.7
2	3	3.5	300	1.5	873	410	53.04	122	21	82.8
3	7	1.5	700	1.5	825	499	39.52	130	29	77.8
4	14	3.5	700	1.5	844	468	44.55	140	10	92.8
5	12	1.5	500	0.5	828	493	40.46	140	28	80
6	8	3.5	500	0.5	888	455	48.76	140	13	90.7
7	1	1.5	500	2.5	844	468	44.55	116	46	60.7
8	17	3.5	500	2.5	888	410	53.83	140	20	85.7
9	6	2.5	300	0.5	865	453	47.63	140	28	80
10	13	2.5	700	0.5	825	499	39.52	124	16	87.1
11	4	2.5	300	2.5	889	455	48.81	142	55	61.4
12	9	2.5	700	2.5	868	482	44.47	122	21	82.8
13	16	2.5	500	1.5	828	451	45.53	142	34	76.1
14	2	2.5	500	1.5	892	485	45.63	119	28	76.4
15	5	2.5	500	1.5	895	467	45.14	124	30	75.8

16	11	2.5	500	1.5	863	461	46.58	130	29	77.8
17	10	2.5	500	1.5	865	466	46.13	119	28	76.4

Legend: VM = magnetizing current, TR = tool rotation, WX = working gap, %SRR = Percentage surface roughness reduction and %RRS = percentage reduction in residual stresses

OUTCOME AND DISCUSSION

Surface roughness and residual stress information is noted at an increment of 10mm for each specimen surface, thus an average of total 5 readings were collected for each workpiece. Percentage surface roughness reduction (%SRR) and residual stress (%RRS) is calculated by equation 1 and 2 respectively.

$$\%SRR = \frac{Initial\ Surface\ Roughness - Final\ Surface\ Roughness}{Initial\ Surface\ Roughness} \times 100 \quad \textbf{(1)}$$

$$\%RRS = \frac{Initial\ Residual\ Stress - Final\ Residual\ Stress}{Initial\ Residual\ Stress} \times 100 \quad \textbf{(2)}$$

Firstly, fitness of the obtained statistical data is to be found i.e. how well the observed data fits with the expected data.

Surface Roughness of Al 7075

Quadratic model was recommended by Design Expert 6.0.8 software for percentage reduction in surface roughness. Table 3 shows the significant parameters or terms. F-value of the model 129.3567 and the corresponding p-value which is less than 0.001 as shown in table 3 indicates that the quadratic model is significant.

An empirical relationship (Equation (3)) between the output response i.e. percentage reduction in surface roughness and input process parameters is acquired after eliminating the non-significant parameters. This equation can be used for obtaining maximum reduction in surface roughness while BEMRF of Al 7075 material by predicting optimal values of input process parameters.

$$\%SRR = 46.13 + 4.50125 * V_M - 2.84625 * T_R + 1.8925 * W_X - 1.635 * T_R^2 + 0.6875 * W_X^2 - 2.1025 * V_M * T_R + 0.94 * T_R * W_X \quad \textbf{(3)}$$

Table 3. ANOVA table for %SRR after eliminating non-significant parameters

Source	Sum of Squares	Degree of Freedom	Mean Square	F Value	Prob > F	
Model	289.5628	7	41.366	129.3567	< 0.0001	Significant
V_M	162.09	1	162.09	506.8745	< 0.0001	Significant
T_R	64.80911	1	64.809	202.6657	< 0.0001	Significant
W_X	28.65245	1	28.652	89.59957	< 0.0001	Significant
T_R^2	11.28695	1	11.287	35.29562	0.0002	Significant
W_X^2	1.99566	1	1.9957	6.240662	0.0340	Significant
$V_M \times T_R$	17.68203	1	17.682	55.29377	< 0.0001	Significant
$T_R \times W_X$	3.5344	1	3.5344	11.05248	0.0089	Significant
Residual	2.87805	9	0.3198			
Lack of Fit	2.02697	5	0.4054	1.905316	0.2760	Not Significant

Pure Error	0.85108	4	0.2128
Cor Total	292.4408	16	

Standard Deviation = 0.565494, R^2 = 0.990159, Adjusted R^2 = 0.982504, Predicted R^2 = 0.946623, Mean = 45.68412, Coefficient of Variance = 1.23784, PRESS = 15.60952, Adequate Precision = 37.88097

Interaction graph of V_M and T_R on %SRR as shown in figure 2(a) clearly explains that %SRR attains a maximum value of 53.94% when V_M is kept at highest level of 3.5A and T_R at lowest value of 300 rpm, keeping W_X constant at 1.5 mm. This is due to the reason that at high level of magnetizing current the normal forces and tangential forces increases which shears more amount of material from the workpiece surface resulting in improved surface finish. On the other hand, a minimum of 39.25% reduction in surface roughness is attained at lowest value (1.5 A) of V_M and highest value (700 rpm) of T_R. This drastic decline in %SRR is due to the fact that at large rotational speed of the tool the quantity of abrasives interacting with workpiece surface through same working gap increases leading to an increase in indentation force. This increase in indentation force results in decrease in surface finish of the workpiece surface.

Combined effect of T_R and W_X on %RRS as represented in figure 2(b) shows that %SRR value increased from 39.5% to 45.17% on increasing W_X from 0.5 to 2.5 mm while keeping T_R at 700 rpm. A significant jump in %SRR value is seen due to the reason that at low W_X more volume of finishing fluid is squeezed between the tip of tool and finishing surface at same tool rotational speed thereby increasing the normal and tangential forces on the surface of the workpiece resulting in poor surface finish. Furthermore, magnetization intensity increases at smaller working gap leading to generation of deep abrasions thus increasing surface roughness. It is also observed that %SRR value further increased to 48.98% from 45.17% once tool rotation value is decreased to 300 rpm, working gap constant at 2.5 mm.

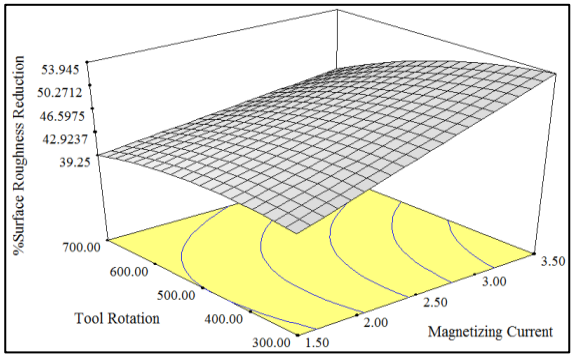

(a)

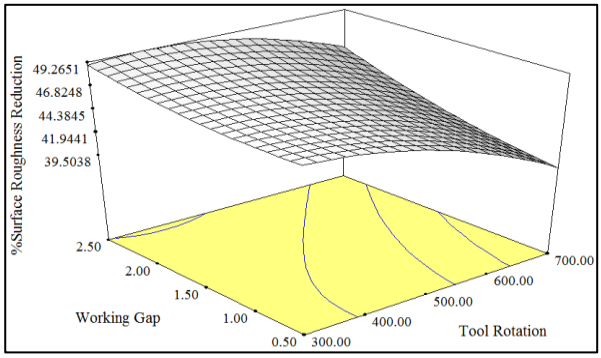

(b)

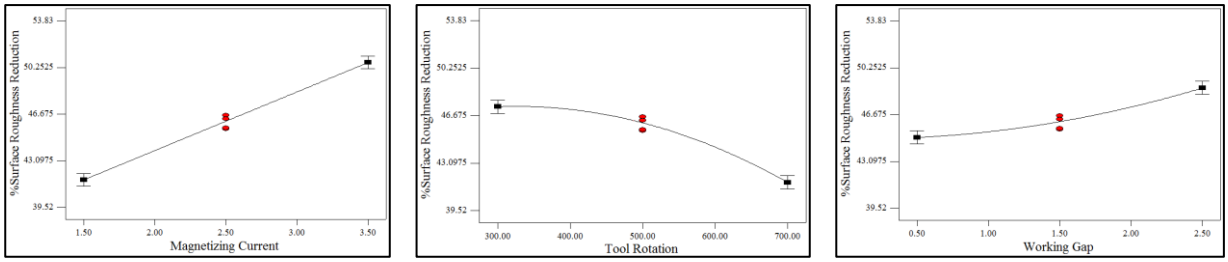

(c) (d) (e)

Figure 2. (a) Interaction graph of V_M & T_R on %SRR, (b) Interaction graph of T_R & W_X on %SRR, (c) Individual effect of V_M on %SRR, (d) Individual effect of T_R on %SRR and (e) Individual effect of W_X on %SRR

Figure 2 (d, e, f) represents the individual impact of magnetizing current, tool rotation and working gap on %SRR respectively. The same slant as the interaction graph was followed by the individual effect plot, which showed that an increase in V_M and W_X increased the %SRR while an increase in T_R reduced %SRR due to the reasons quoted above. Surface finish is an important constraint to assess the materials functional performance. Ghosh (2018) concluded that the optical materials to be utilised in optical industries are expected to acquire nanometric finish without any surface or sub-surface damage.

Residual Stress on Al 7075

Figure 3 represents the residual stresses on aluminium 7075 workpiece obtained after BEMRF process keeping magnetizing current, tool rotation and working gap at 1.5 mm, 3.5 amp, 700 rpm respectively. A maximum of 92.8 percentage reduction in residual stress is obtained at above mentioned parametric values. Table 4 shows the significant parameters or terms. F-value of the model 133.6858 and the corresponding p-value which is less than 0.001 as shown in table 4 indicates that the quadratic model is significant.

An empirical relationship (Equation (4)) between the output response i.e. percentage reduction in residual stress and input process parameters is acquired after eliminating the non-significant parameters. This equation can be used for obtaining maximum reduction in residual stress while BEMRF of Al7075 material by predicting optimal values of input process parameters.

$$\%RRS = 75.88888889 + 9.45 * V_M + 7.65 * T_R - 5.95 * W_X + 2.586111111 * C^2 - 1.925 * V_M * T_R + 3.875 * V_M * W_X + 3.425 * T_R * W_X \quad \textbf{(4)}$$

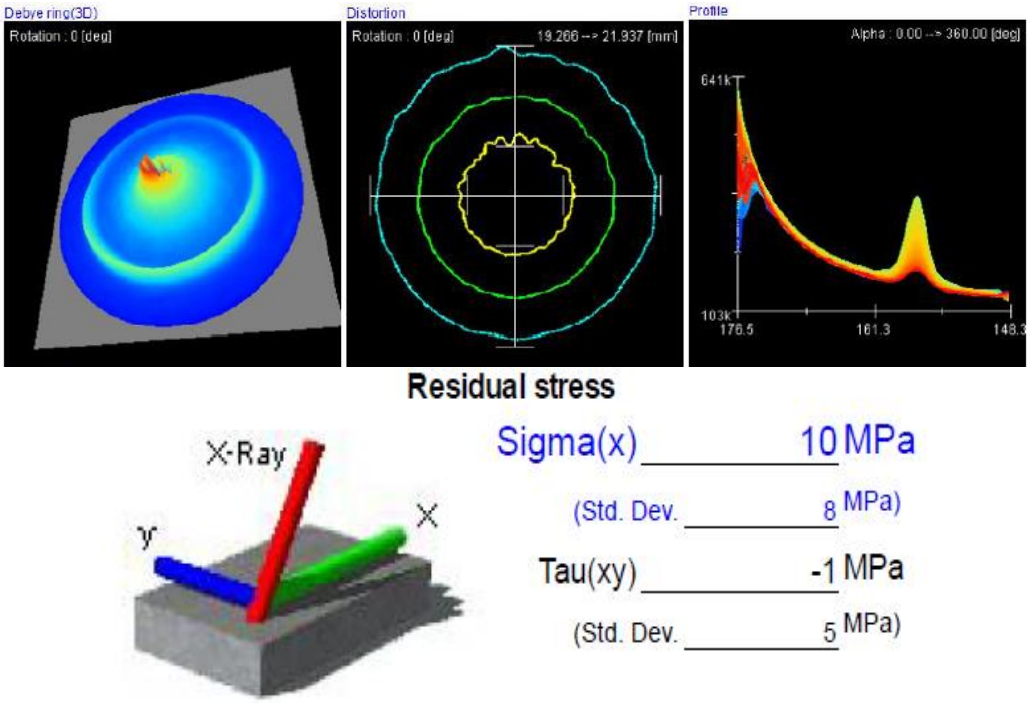

Figure 3. Residual stress on aluminium 7075 workpiece after BEMRF

Table 4. ANOVA table for %RRS after eliminating non-significant parameters

Source	Sum of Squares	Degree of Freedom	Mean Square	F Value	Prob > F	
Model	1646.11	7	235.159	133.6858	< 0.0001	Significant
V_M	756.605	1	756.605	430.123	< 0.0001	Significant
T_R	459.045	1	459.045	260.9629	< 0.0001	Significant
W_X	278.480	1	278.480	158.3133	< 0.0001	Significant
W_X^2	13.1358	1	13.1358	7.467592	0.0231	Significant
$V_M \times T_R$	36.6025	1	36.6025	20.80819	0.0014	Significant
$V_M \times W_X$	51.1225	1	51.1225	29.06267	0.0004	Significant
$T_R \times W_X$	51.1225	1	51.1225	29.06267	0.0004	Significant
Residual	15.8314	9	1.75904			
Lack of Fit	12.8914	5	2.57828	3.507861	0.1239	Not Significant
Pure Error	2.94000	4	0.73500			
Cor Total	1661.95	16				

Standard Deviation = 1.326289, R^2 = 0.990474, Adjusted R^2 = 0.983065, Predicted R^2 = 0.946557, Mean = 77.61765, Coefficient of Variance = 1.70875, PRESS = 88.8201, Adequate Precision = 38.02

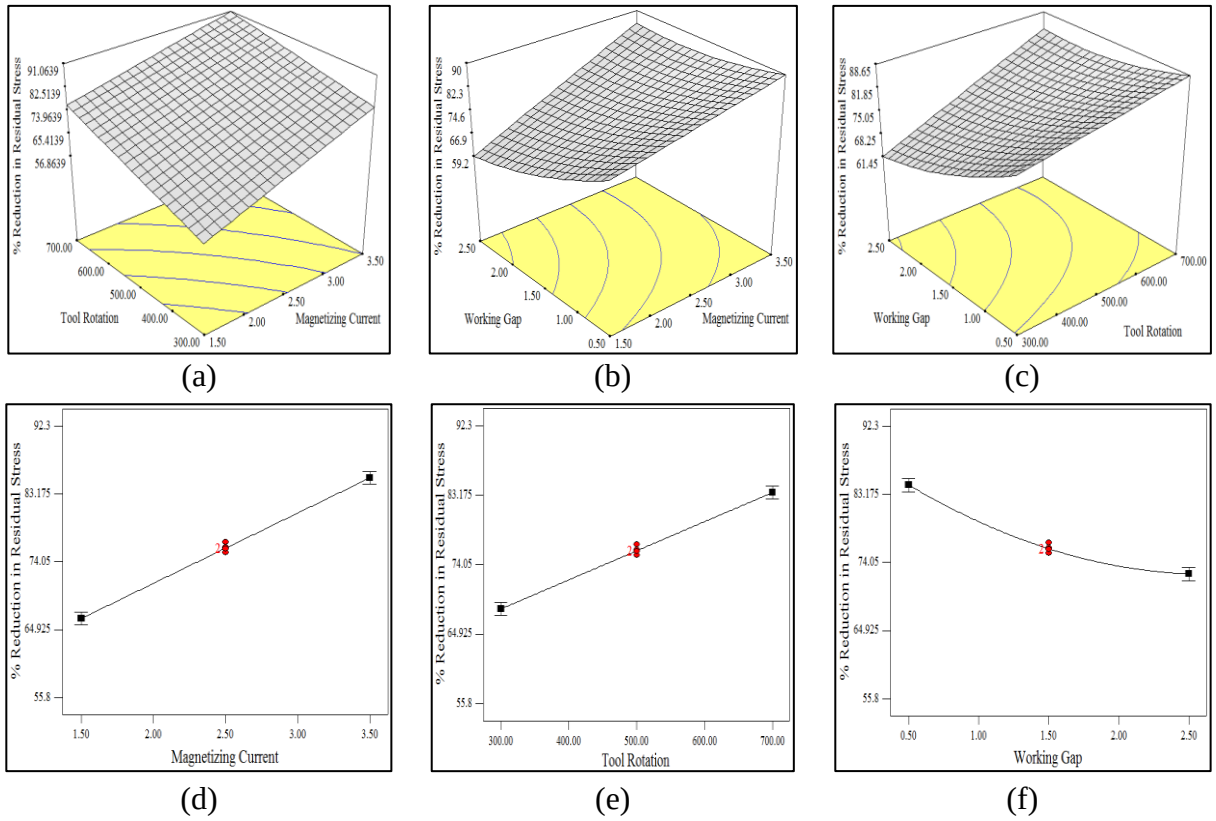

Figure 4. (a) Interaction graph of V_M and T_R on %RRS, (b) Interaction graph of V_M and W_X on %RRS, (c) Interaction graph of T_R and W_X on %RRS, (d) Individual effect of V_M on %RRS, (e) Individual effect of W_X on %RRS

Combined effect of T_R and W_X on %RRS as represented in figure 4(c) shows that %RRS value reduced from 80.2% to 61.45% on increasing W_X from 0.5 to 2.5 mm while keeping T_R at 300 rpm. Whereas, on increasing T_R from 300 to 700 rpm and keeping W_X constant at 2.5 mm, the percentage reduction in residual stress drastically increased to a high value of 83.6%. On the other hand, keeping T_R at maximum value of 700 rpm and reducing W_X to the lowest value of 0.5 mm results in increase of percentage reduction in residual stress to a value of 88.65%. It was observed that with a surge in tool rotation and simultaneous decrement in working gap, the residual stress increases as the workpiece experiences shear and Hertzian stress owing to the vibrations with the abrasive particles.

Figure 4 (d, e, f) shows the individual impact of V_M, T_R and W_X on %RRS. The same slant as the interaction graph was followed by the individual effect plot, which showed that an increase in V_M and T_R increased the %RRS while an increase in W_X reduced the %RRS.

OUTPUT RESPONSE OPTIMIZATION

Derringer (1980) introduced a desirability function approach that was applied to optimize the response to the output i.e. percentage surface reduction (%SRR) and percentage reduction in residual stress (%RRS). In this approach, the measured properties of each predicted response where d ranges between 0 and 1 are assigned a dimensionless desirability value (d). Montgomery

(2001) described that if the desirability function reaches a value of 0 it refers to an unacceptable response and if d = 1 then the answer is exactly to the destination. As the desirability of the corresponding response increases the value of d increases. In the present work, the scenario considered is larger the better rate of cutting. The equation given below is used to transform the response into a dimensionless function di.

$$d_i = \begin{cases} 0 & Xi < Bi \\ (Xi - Bi/Hi - Bi)^w & Bi \leq Mi \leq Hi \\ 1 & Bi > Hi \end{cases} \quad \textbf{(5)}$$

where Bi = Lower response limit, Mi = Upper response limit, Hi = Response goal value. B and M are selected in RSM according to the mathematical.

Optimization Steps:

- Finding the desirability response value
- Optimizing desirability function and detecting the best possible response value

Table 5 shows the top 10 solutions achieved using desirability method after response optimization. A highest desirability value of 0.95 is obtained after optimization which means that maximum percentage reduction in surface roughness and residual stress value can be obtained at V_M = 3.5 amp, T_R = 300 rpm and W_X = 0.5 mm while finishing of aluminium 7075 through BEMRF process.

Table 5. Top 10 predicted solutions using desirability method

Solution Number	Magnetizing Current	Tool Rotation	Working Gap	% Surface Roughness Reduction	% Reduction in Residual Stress	Desirability	
1	**3.50**	**300.00**	**0.50**	**53.680**	**89.6249**	**0.951226**	**Selected**
2	**3.49**	**300.01**	**0.50**	**53.615**	**89.5343**	**0.947760**	**Selected**
3	3.50	300.02	0.53	53.669	89.3828	0.947468	
4	3.50	311.46	0.50	53.524	89.6808	0.946769	
5	3.41	300.04	0.50	53.091	88.8078	0.919958	
6	3.50	300.00	0.79	53.615	87.0794	0.912754	
7	3.50	487.43	2.50	53.457	85.4392	0.883565	
8	3.50	495.32	2.50	53.304	85.7601	0.883439	
9	3.50	502.38	2.50	53.163	86.0465	0.883097	
10	3.50	471.75	2.50	53.745	84.8023	0.883041	

In order to check the above solutions a confirmatory experiment was conducted for solution no. 1 and 2. The values of the input process parameters in table 5 are rounded to the nearest integer

value and the results of the confirmatory experiments mentioned in table 6 indicates that less than 2% of error was obtained. These results confirm excellent reproducibility of the favorable solutions obtained after the optimization.

Table 6. Confirmatory experiments

Solution Number	Magnetizing Current	Tool Rotation	Working Gap	Predicted		Actual		Error %	Error %
				%RRS	%SRR	%RRS	%SRR	%RRS	%SRR
1	3.50	300	0.5	89.6249	53.680	90.7811	54.2329	-1.29	-1.03
2	3.50	300	0.5	89.5343	53.615	89.6686	53.7544	-0.15	-0.26

CONCLUSION

This research work explores the minimization of surface roughness and residual stresses induced after grinding process on Al 7075 workpiece surface through polishing using BEMRF process. The effects of input constraints viz. magnetizing current, tool rotation and working gap were studied through variation in percentage surface roughness reduction (%SRR) and percentage reduction in residual stresses (%RRS). Desirability approach was used to carry out the optimization of %SRR and %RRS through design expert software. From this study, following conclusions are drawn.

- All the input process parameters had a significant effect on both the output responses viz. percentage surface roughness reduction and percentage reduction in residual stress during the BEMRF process.
- Although according to ANOVA table, combined impact of magnetizing current and tool rotation and collective effect of tool rotation and working gap on percentage surface roughness reduction was found to be significant.
- It was found that the %SRR increased from 41.63% to 50.63% when magnetizing current value was increased from 1.5 A to 3.5 A keeping tool rotation and working gap constant at 500 rpm and 1.5 mm respectively.
- Results also showed that the percentage reduction in surface roughness decreased to 41.65% from 47.34% when tool rotation increased to highest level of 700 rpm.
- Although according to ANOVA table, effect of W_X was found to be significant on %SRR but only 3.78% increase was observed when W_X was increased from 0.5 to 2.5 mm.
- Also, combined impact of magnetizing current and tool rotation, magnetizing current and working gap and tool rotation and working gap on percentage reduction in residual stress was found to be significant.

- Results showed that the % reduction in residual stress value elevated from 60.44 to 85.34% when magnetizing current was increased from 1.5 to 3.5 amp.
- It was observed that on increasing tool rotation from 300 to 700 rpm, the percentage reduction in residual stress value was increased to 83.54% from 68.24%.
- Results also showed that on increasing working gap to the highest level (2.5 mm) the percentage reduction in residual stressed decreased to 72.53% from 84.43%.

FUTURE SCOPE

There are various areas of future research depending on the current mentioned technique. Some of the areas to engage in are nano level finishing of nanocomposite materials (Qi et al., 2021; Wu et al. 2021 & Wu et al. 2020), ceramics (Sun et al. 2021) and also comparing two or more nano level finishing techniques like MRAFF, CMMRF etc.

REFERENCES

Ahn, Y., Yoon, J. Y., Baek, C. W., & Kim, Y. K., 2004. Chemical mechanical polishing by colloidal silica-based slurry for micro-scratch reduction. *Wear*, *257*(7-8), 785-789., https://doi.org/10.1016/j.wear.2004.03.020.

Arrasmith, S. R., Jacobs, S. D., Lambropoulos, J. C., Maltsev, A., Golini, D., & Kordonski, W. I., 2001, December. Use of magnetorheological finishing (MRF) to relieve residual stress and subsurface damage on lapped semiconductor silicon wafers. In *Optical manufacturing and testing IV* (Vol. 4451, pp. 286-294). International Society for Optics and Photonics.

Arun, A., Malrautu, P., Laha, A., & Ramakrishna, S., 2021. Gelatin Nanofibers in Drug Delivery Systems and Tissue Engineering. *Engineered Science*, *16*, 71-81.

Brinksmeier, E., 1987. A model for the development of residual stresses in grinding. In *Advances in Surface Treatments* (pp. 173-189). Pergamon.

Brinksmeier, E., Sölter, J., & Grote, C., 2007. Distortion engineering–identification of causes for dimensional and form deviations of bearing rings. *CIRP annals*, *56*(1), 109-112.

Chiu, S. Y., Wang, Y. L., Liu, C. P., Lan, J. K., Ay, C., Feng, M. S., ... & Dai, B. T., 2003. The application of electrochemical metrologies for investigating chemical mechanical polishing of Al with a Ti barrier layer. *Materials chemistry and physics*, *82*(2), 444-451., https://doi.org/10.1016/S0254-0584(03)00312-2.

Derringer, G., & Suich, R., 1980. Simultaneous optimization of several response variables. *Journal of quality technology*, *12*(4), 214-219.

Ghosh, G., Sidpara, A., & Bandyopadhyay, P. P., 2018. Fabrication of optical components by ultraprecision finishing processes. In *Micro and Precision Manufacturing* (pp. 87-119). Springer, Cham.

Ghosh, G., Sidpara, A., & Bandyopadhyay, P. P., 2021. Experimental and theoretical investigation into surface roughness and residual stress in magnetorheological finishing of OFHC copper. *Journal of Materials Processing Technology*, *288*, 116899.

Golini, D., Jacobs, S. D., Kordonski, W. I., & Dumas, P., 1997, July. Precision optics fabrication using magnetorheological finishing. In *Advanced Materials for Optics and Precision Structures: A Critical Review* (Vol. 10289, p. 102890H). International Society for Optics and Photonics

Jacobs, S. D., Golini, D., Hsu, Y., Puchebner, B. E., Strafford, D., Prokhorov, I. V., ... & Kordonski, W. I., 1995. Magnetorheological finishing: a deterministic process for optics manufacturing. In *International Conference on Optical Fabrication and Testing* (Vol. 2576, pp. 372-383). International Society for Optics and Photonics

Jaecklin, V. P., Linder, C., Brugger, J., De Rooij, N. F., Moret, J. M., & Vuilleumier, R., 1994. Mechanical and optical properties of surface micromachined torsional mirrors in silicon, polysilicon and aluminum. *Sensors and Actuators A: Physical*, *43*(1-3), 269-275., https://doi.org/10.1016/0924-4247(93)00699-5.

Jain, V. K., Ranjan, P., Suri, V. K., & Komanduri, R., 2010. Chemo-mechanical magneto-rheological finishing (CMMRF) of silicon for microelectronics applications. *CIRP Annals-Manufacturing Technology*, *59*(1), 323-328

Jha, S., & Jain, V. K., 2004. Design and development of the magnetorheological abrasive flow finishing (MRAFF) process. International Journal of Machine Tools and Manufacture, 44(10), 1019-1029

Jomaa, W., Songmene, V., & Bocher, P., 2014. Surface finish and residual stresses induced by orthogonal dry machining of AA7075-T651. Materials, 7(3), 1603-1624.

Kansal, H., Singh, A. K., & Grover, V., 2018. Magnetorheological nano-finishing of diamagnetic material using permanent magnets tool. *Precision Engineering*, *51*, 30-39.

Khan, D. A., & Jha, S., 2018. Synthesis of polishing fluid and novel approach for nanofinishing of copper using ball-end magnetorheological finishing process. *Materials and Manufacturing Processes*, *33*(11), 1150-1159

Khan, D. A., & Jha, S., 2019. Selection of optimum polishing fluid composition for ball end magnetorheological finishing (BEMRF) of copper. The International Journal of Advanced Manufacturing Technology, 100(5-8), 1093-1103.

Kruszynski, B. W., & Van Luttervelt, C. A., 1991. An attempt to predict residual stresses in grinding of metals with the aid of a new grinding parameter. *CIRP annals*, *40*(1), 335-337.

Lambropoulos, J. C., Arrasmith, S. R., Jacobs, S. D., & Golini, D., 2001, December. Manufacturing-induced residual stresses in optical glasses and crystals: Example of residual stress relief by magnetorheological finishing (MRF) in commercial silicon wafers. In *Optical Manufacturing and Testing IV* (Vol. 4451, pp. 181-190). International Society for Optics and Photonics.

Li, Q.Y., Hao, Q., Zhu, T., & Zebarjadi, M., 2020. Nanostructured and heterostructured 2D materials for thermoelectrics. *Engineered Science*, 13, 24-50.

Mahadik, S.A., Patil, A., Pathan, H.M., Salunke-Gawali, S., & Butcher, R.J., 2020. Thionaphthoquinones as Photosensitizers for TiO2 Nanorods and ZnO Nanograin Based Dye-sensitized Solar Cells: Effect of Nanostructures on Charge Transport and Photovoltaic Performance. *Engineered Science*, *14*, 46-58.

Maloney, C., Lormeau, J. P., & Dumas, P., 2016, June. Improving low, mid and high-spatial frequency errors on advanced aspherical and freeform optics with MRF. In *Third European Seminar on Precision Optics Manufacturing* (Vol. 10009, p. 100090R). International Society for Optics and Photonics.

Montgomery, D.C., 2001. Design and Analysis of Experiments, John Wiley & Sons Inc. New York.

Qi, G., Liu, Y., Chen, L., Xie, P., Pan, D., Shi, Z., ... & Guo, Z., 2021. Lightweight Fe3C@ Fe/C nanocomposites derived from wasted cornstalks with high-efficiency microwave absorption and ultrathin thickness. *Advanced Composites and Hybrid Materials*, *4*(4), 1226-1238.

Qiu, Y., Xu, M., Li, Q., Huang, R., & Wang, J., 2021. A high-temperature near-perfect solar selective absorber combining tungsten nanohole and nanoshuriken arrays. *ES Energy & Environment*, *13*, 77-90.

RKoul, R., AMitra, A., & VChitnis, T., 2011. An update on the design and implementation of the MACE gamma-ray telescope. In *International Cosmic Ray Conference* (Vol. 9, p. 106)., https://doi.org/10.7529/ICRC2011/V09/0803.

Robinson, J. S., Hossain, S., Truman, C. E., Paradowska, A. M., Hughes, D. J., Wimpory, R. C., & Fox, M. E., 2010. Residual stress in 7449 aluminium alloy forgings. *Materials Science and Engineering: A*, *527*(10-11), 2603-2612.

Saraswathamma, K., Jha, S., & Rao, P. V., 2015. Experimental investigation into ball end magnetorheological finishing of silicon. *Precision Engineering*, *42*, 218-223.

Sharma, A., & Niranjan, M.S., 2019. Magnetorheological Fluid Finishing of Soft Materials: A Critical Review. International journal of advanced production and industrial engineering, Vol 4 (1), 48-55.

Sharma, A., Vaish, A. & Sharma, A., 2020. Detailed Review of Ball End Magnetorheological Fluid Finishing Process. WSEAS TRANSACTIONS on HEAT and MASS TRANSFER, Vol 15, 163-173.

Sim, W. M., 2010. Challenges of residual stress and part distortion in the civil airframe industry. *International Journal of Microstructure and Materials Properties*, *5*(4-5), 446-455.

Singh, A. K., Jha, S., & Pandey, P. M., 2012. Magnetorheological ball end finishing process. *Materials and Manufacturing Processes*, *27*(4), 389-394.

Singh, A. K., Jha, S., & Pandey, P. M., 2012. Nanofinishing of fused silica glass using ball-end magnetorheological finishing tool. *Materials and Manufacturing Processes*, *27*(10), 1139-1144.

Sugano, T., Takeuchi, K., Goto, T., Yoshida, Y., Ikawa, N., 1987. Diamond turning of an aluminum alloy for mirror. CIRP Ann. Manuf. Technol. 36 (1), 17–20.

Sun, Z., Huang, X., Xia, A., Yan, Z., & Qian, L., 2021. Tunable Bandwidth of Negative Permittivity from Graphene-Silicon Carbide Ceramics. *Engineered Science*, *16*, 19-25.

Tönshoff, H. K., Peters, J., Inasaki, I., & Paul, T., 1992. Modelling and simulation of grinding processes. *CIRP annals*, *41*(2), 677-688.

Tyagi, P., & Vedeshwar, A. G., 2002. Effect of residual stress on the optical properties of CdI 2 films. *Physical Review B*, *66*(7), 075422.

Vahdati, M., & Shokuhfar, A., 2008. A trend toward abrasive nano finishing of plane surfaces with magnetic field energy. Materialwissenschaft und Werkstofftechnik, 39(2), 167-170.

Wu, H., Zhong, Y., Tang, Y., Huang, Y., Liu, G., Sun, W., ... & Guo, Z. 2021. Precise regulation of weakly negative permittivity in CaCu3Ti4O12 metacomposites by synergistic effects of carbon nanotubes and grapheme. *Advanced Composites and Hybrid Materials*, 1-12.

Wu, N., Du, W., Hu, Q., & Jiang, S.V.Q., 2020. Recent development in fabrication of Co nanostructures and their carbon nanocomposites for electromagnetic wave absorption. *Engineered Science*, *13*(13), 11-23.

Yi, A. Y., Tao, B., Klocke, F., Dambon, O., & Wang, F., 2011. Residual stresses in glass after molding and its influence on optical properties. *Procedia Engineering*, *19*, 402-406

Zhejun, Y., Zhonghui, H., & Kobayashi, A., 1989. Surface integrity of grinding of bearing steel GCr15 with CBN wheels. *CIRP annals*, *38*(1), 553-556.
Zhong, Z.W., Lu, Y.G., 2003. Fractal roughness structure of diamond-turned copper mirrors. Mater. Manuf. Process. 18 (2), 219–227.